

Electronic states and transport properties in the Kronig-Penney model with correlated compositional and structural disorder

J. C. Hernández-Herrejón¹, F. M. Izrailev², and L. Tessieri¹

¹ *Instituto de Física y Matemáticas*

Universidad Michoacana de San Nicolás de Hidalgo

Morelia, Mich., 58060, Mexico

² *Instituto de Física, Universidad Autónoma de Puebla,*

Puebla, Pue., 72570, Mexico

15th March 2010

Abstract

We study the structure of the electronic states and the transport properties of a Kronig-Penney model with weak compositional and structural disorder. Using a perturbative approach we obtain an analytical expression for the localisation length which is valid for disorder with arbitrary correlations. We show how to generate disorder with self- and cross-correlations and we analyse both the known delocalisation effects of the long-range self-correlations and new effects produced by cross-correlations. We finally discuss how both kinds of correlations alter the transport properties in Kronig-Penney models of finite size.

Pacs: 73.20.Jc, 73.20.Fz, 71.23.An

1 Introduction

The recent surge of interest in one-dimensional disordered models can be attributed in large part to the realisation that long-range correlations of

the random potentials can significantly alter the structure of the electronic states, enhancing or suppressing their localisation in continuous intervals of energy [1, 2, 3, 4, 5]. This discovery has paved the way for the construction of one-dimensional electronic, optical or electromagnetic devices with anomalous transport properties. Specifically, it is now possible to design filters with almost perfect transmission or reflection in pre-defined energy windows. This possibility, first foreseen at the theoretical level [2, 3], was later confirmed experimentally [4, 5].

The periodic Kronig-Penney model was originally introduced in the early 1930s to analyse the electronic states and the energy bands in crystalline structures [6]. In the 1980s the model was used to describe semiconductor superlattices (see [7] and references therein). More recently, aperiodic variants of the Kronig-Penney model were used to analyse the transmission properties of a waveguide with long-range correlated compositional [4, 5] or structural [8] disorder. The wide applicability of aperiodic Kronig-Penney models makes desirable to analyse in full detail the structure of their electronic states. Two kinds of disorder are typically considered in the aperiodic Kronig-Penney model: structural and compositional disorder. In the first case the positions of potential barriers are randomised; thus, they do not coincide with the sites of the underlying lattice. In the second case the disorder is introduced by assigning random heights or widths to the potential barriers.

In this paper we study a Kronig-Penney model with delta-shaped potential barriers with weak correlated disorder of both the compositional and structural type. This model was first analysed in [9], where we presented an analytical expression for the inverse localisation length valid for any kind of self- and cross-correlations of the two disorders. Here we give a detailed derivation of this result, together with an extended discussion of various physical implications. In particular, we describe how to construct two sequences of random variables, representing the positions and strengths of the barriers, with arbitrary self- and cross-correlations. We show that specific long-range self-correlations can create a delocalisation-localisation transition (within the limit of the second-order perturbative approach) and we analyse new effects produced by the cross-correlations of the two kinds of disorder. We then discuss how the both kinds of correlations affect the electronic transport properties in finite samples.

This paper is organised as follows. In Sec. 2 we define the model under study and derive an analytical expression for the electronic localisation length

using the Hamiltonian map approach. In Sec. 3 we show how to construct sequences of correlated random variables for the positions and strengths of the barriers. We also demonstrate how the localisation/delocalisation effects produced by long-range self-correlations of the disorder are modified by the cross-correlations. In Sec. 4 we analyse how these effects alter the transport properties of finite-size models. The conclusions are drawn in Sec. 5.

2 Structure of the electronic states

2.1 Definition of the model

Here we define the Kronig-Penney model with weak compositional and structural disorder. The model describes the motion of an electron in a succession of delta-shaped barriers; disorder is introduced by assuming that both the strength and the position of each barrier are random variables fluctuating around their average values. The corresponding Schrödinger equation is

$$-\psi''(x) + \left[\sum_{n=-\infty}^{\infty} U_n \delta(x - d_n) \right] \psi(x) = q^2 \psi(x) \quad (1)$$

with the electron energy given by the square of the propagation wavevector within the wells

$$E = q^2. \quad (2)$$

In Eqs. (1) and (2) we have used units such that $\hbar^2/2m = 1$; we will stick to this choice throughout this paper.

In the model (1) the delta-barriers are located at the points $d_n = na + a_n$, where the random shifts a_n with respect to the lattice sites na represent the structural (or *positional*) disorder. The compositional (or *amplitude*) disorder, on the other hand, enters via $U_n = U + u_n$, with the random variables u_n corresponding to fluctuations of the barrier strengths around their mean value U .

We define the statistical properties of the model in terms of the strength fluctuations u_n and of the relative barrier displacements $\Delta_n = a_{n+1} - a_n$ (which turn out to be more relevant than the absolute displacements a_n themselves). We restrict our attention to the weak-disorder case, defined by the conditions

$$\langle u_n^2 \rangle \ll U^2 \quad (3)$$

and

$$\langle \Delta_n^2 \rangle q^2 \ll 1 \quad \text{and} \quad \langle \Delta_n^2 \rangle U \ll 1. \quad (4)$$

The condition (3) implies that the compositional disorder is weak in the sense that the fluctuations of the barrier strength are small with respect to their mean value. The weakness of structural disorder is defined by the condition (4), which requires that the relative displacements of the barriers should be small on the length scales set by $1/q$ and $1/\sqrt{U}$.

In the weak-disorder case the statistical properties of the model can be analysed in terms of the averages and of the binary correlators of the random variables u_n and Δ_n . Both variables are assumed to have zero mean. In what follows we consider the normalised binary correlators

$$\begin{aligned} \chi_1(k) &= \frac{\langle u_n u_{n+k} \rangle}{\langle u_n^2 \rangle} \\ \chi_2(k) &= \frac{\langle \Delta_n \Delta_{n+k} \rangle}{\langle \Delta_n^2 \rangle} \\ \chi_3(k) &= \frac{\langle u_n \Delta_{n+k} \rangle}{\langle u_n \Delta_n \rangle} \end{aligned} \quad (5)$$

as given functions. We do not attribute any specific form to the correlators (5); we only suppose that they are even functions of the index difference as a consequence of the assumed spatial isotropy and homogeneity in the mean of the model.

2.2 The Hamiltonian map

The electronic states of the Kronig-Penney model (1) can be analysed by means of the Hamiltonian map approach. This approach is based on the mathematical identity of the Schrödinger equation (1) with the dynamical equation of a classical oscillator with noisy frequency [10, 11]. The stochastic oscillator corresponding to the Kronig-Penney model is defined by the Hamiltonian

$$H = \frac{p^2}{2} + \frac{1}{2} \left\{ q^2 - \left[\sum_{n=-\infty}^{\infty} U_n \delta(t - na + a_n) \right] \right\} x^2. \quad (6)$$

with the electron wavevector q playing the role of the unperturbed frequency. The mathematical analogy between the Schrödinger equation (1) and the

dynamical equation of the parametric oscillator (6) allows one to analyse the behaviour of the electronic states of the Kronig-Penney model in terms of the trajectories of the kicked oscillator. This dynamical approach implies that the Schrödinger equation is solved as an initial-value problem; hence the Hamiltonian map method is equivalent to the transfer matrix technique.

Given the Hamiltonian (6), one can integrate the corresponding dynamical equations over the time interval $[d_n^-, d_{n+1}^-]$ between two kicks. In this way one obtains the Hamiltonian map

$$\begin{pmatrix} x_{n+1} \\ p_{n+1} \end{pmatrix} = \mathbf{T}_n \begin{pmatrix} x_n \\ p_n \end{pmatrix} \quad (7)$$

with the transfer matrix

$$\mathbf{T}_n = \begin{pmatrix} \cos[q(a + \Delta_n)] + (U + u_n) \frac{1}{q} \sin[q(a + \Delta_n)] & \frac{1}{q} \sin[q(a + \Delta_n)] \\ -q \sin[q(a + \Delta_n)] + (U + u_n) \cos[q(a + \Delta_n)] & \cos[q(a + \Delta_n)] \end{pmatrix}. \quad (8)$$

To analyse the trajectories of the Hamiltonian map (7), we follow the approach proposed in [3]. Specifically we perform a canonical transformation $(x_n, p_n) \rightarrow (X_n, P_n)$ such that the unperturbed motion reduces to a simple rotation in the new variables. The appropriate canonical transformation has the form

$$\begin{pmatrix} x_n \\ p_n \end{pmatrix} = \mathbf{M} \begin{pmatrix} X_n \\ P_n \end{pmatrix} \quad (9)$$

with

$$\mathbf{M} = \begin{pmatrix} \alpha \cos \frac{qa}{2} & \frac{1}{q\alpha} \sin \frac{qa}{2} \\ -q\alpha \sin \frac{qa}{2} & \frac{1}{\alpha} \cos \frac{qa}{2} \end{pmatrix}$$

where the parameter α is defined by the relation

$$\alpha^4 = \frac{1}{q^2} \frac{\sin(qa) - \frac{U}{2q} [\cos(qa) - 1]}{\sin(qa) - \frac{U}{2q} [\cos(qa) + 1]}. \quad (10)$$

Note that the canonical transformation (9) rescales time so that the new coordinate X_n and the corresponding conjugate momentum P_n have the same dimensions.

Since we are interested only in the weak-noise case, we can expand the new transfer matrix $\tilde{\mathbf{T}}_n = \mathbf{M}^{-1}\mathbf{T}_n\mathbf{M}$ and keep only terms up to the second order. The Hamiltonian map then takes the form

$$\begin{pmatrix} X_{n+1} \\ P_{n+1} \end{pmatrix} = [\tilde{\mathbf{T}}_n^{(0)} + \tilde{\mathbf{T}}_n^{(1)} + \tilde{\mathbf{T}}_n^{(2)} + o(2)] \begin{pmatrix} X_n \\ P_n \end{pmatrix} \quad (11)$$

where, as desired, the unperturbed matrix represents a rotation

$$\tilde{\mathbf{T}}_n^{(0)} = \mathbf{M}^{-1}\mathbf{T}_n^{(0)}\mathbf{M} = \begin{pmatrix} \cos(ka) & \sin(ka) \\ -\sin(ka) & \cos(ka) \end{pmatrix},$$

with the rotation angle ka being defined by the equation

$$\cos(ka) = \cos(qa) + \frac{U}{2q} \sin(qa). \quad (12)$$

In terms of the Kronig-Penney model, k is the Bloch wavevector, while equation (12) defines the band structure of the model. The explicit form of the first- and the second-order terms of the map (11) is

$$\tilde{\mathbf{T}}_n^{(1)} = \begin{pmatrix} \frac{\sin(qa)}{2q}u_n - \frac{1}{\alpha^2}\sin(ka)\Delta_n & \frac{1}{\alpha^2}\left[\frac{1 - \cos(qa)}{2q^2}u_n - \cos(ka)\Delta_n\right] \\ \alpha^2q^2\left[\frac{1 + \cos(qa)}{2q^2}u_n - \cos(ka)\Delta_n\right] & \frac{\sin(qa)}{2q}u_n - \alpha^2q^2\sin(ka)\Delta_n \end{pmatrix}$$

and

$$\tilde{\mathbf{T}}_n^{(2)} = \begin{pmatrix} \frac{\cos(qa) + 1}{2}u_n\Delta_n - \frac{1}{2}q^2\cos(ka)\Delta_n^2 & \frac{\sin(qa)}{2q\alpha^2}u_n\Delta_n - \frac{1}{2}q^2\sin(ka)\Delta_n^2 \\ -\frac{q\alpha^2}{2}\sin(qa)u_n\Delta_n + \frac{1}{2}q^2\sin(ka)\Delta_n^2 & \frac{\cos(qa) - 1}{2}u_n\Delta_n - \frac{1}{2}q^2\cos(ka)\Delta_n^2 \end{pmatrix}.$$

A remark is in order here. The canonical transformation (9) is well-defined for every value of the rotation angle ka *except* for the critical values $ka = 0$ and $ka = \pm\pi$. In terms of the Kronig-Penney model, this means that our approach fails at the centre and at the edges of the first Brillouin zone. This can be seen by considering that Eq. (12) implies that

$$\sin(ka) = \pm \sqrt{\left\{\sin(qa) - \frac{U}{2q}[\cos(qa) + 1]\right\} \left\{\sin(qa) - \frac{U}{2q}[\cos(qa) - 1]\right\}}.$$

This identity shows that, whenever the sine of the rotation angle is equal to zero, the α parameter (10) either vanishes or diverges. In both cases the canonical transformation (9) is not properly defined, because some elements of the matrix \mathbf{M} diverge. However, we would like to stress that the canonical transformation is perfectly well-defined as long as the rotation angle is arbitrarily close (but not exactly identical) to the singular values $ka = 0$ and $ka = \pm\pi$. Hence our approach works well in every neighbourhood of these critical points.

To analyse the evolution of the dynamical system (11), it is convenient to switch from Cartesian to action-angle coordinates, defined via the equations

$$\begin{aligned} X_n &= \sqrt{2J_n} \sin \theta_n \\ P_n &= \sqrt{2J_n} \cos \theta_n \end{aligned}.$$

In terms of the new variables, the Hamiltonian map (11) takes the form

$$\begin{aligned} J_{n+1} &= D_n^2 J_n \\ \theta_{n+1} &= \theta_n + ka - \frac{1}{2} [1 - \cos(2\theta_n + ka)] \tilde{u}_n + \frac{1}{2} [\zeta - \cos(2\theta_n + 2ka)] \tilde{\Delta}_n \\ &\quad + \frac{1}{8} [2 \sin(2\theta_n + ka) - \sin(4\theta_n + 2ka)] \tilde{u}_n^2 \\ &\quad + \frac{1}{8} [2\zeta \sin(2\theta_n + 2ka) - \sin(4\theta_n + 4ka)] \tilde{\Delta}_n^2 \\ &\quad + \frac{1}{4} [\sin(ka) - 2 \sin(2\theta_n + 2ka) + \sin(4\theta_n + 3ka)] \tilde{u}_n \tilde{\Delta}_n, \end{aligned} \tag{13}$$

with the ratio of the action variables being equal to

$$\begin{aligned} D_n^2 &= 1 + \sin(2\theta_n + ka) \tilde{u}_n - \sin(2\theta_n + 2ka) \tilde{\Delta}_n \\ &\quad + \frac{1}{2} [1 - \cos(2\theta_n + ka)] \tilde{u}_n^2 + \frac{1}{2} [1 - \zeta \cos(2\theta_n + 2ka)] \tilde{\Delta}_n^2 \\ &\quad + [\cos(2\theta_n + 2ka) - \cos(ka)] \tilde{u}_n \tilde{\Delta}_n. \end{aligned} \tag{14}$$

In Eqs. (13) and (14) we made use of the rescaled random variables

$$\tilde{u}_n = \frac{\sin(qa)}{q \sin(ka)} u_n \quad \text{and} \quad \tilde{\Delta}_n = \frac{U}{\sin(ka)} \Delta_n \tag{15}$$

and we introduced the short-hand notation

$$\zeta = \frac{q \sin(ka)}{U} \left[q\alpha^2 + \frac{1}{q\alpha^2} \right]. \tag{16}$$

We remark that the angle variable evolves independently of the action variable.

2.3 The localisation length

This subsection is devoted to the task of evaluating the localisation length in the Kronig-Penney model (1). The inverse localisation length is defined as

$$l_{\text{loc}}^{-1} = \lim_{N \rightarrow \infty} \frac{1}{Na} \sum_{n=1}^N \log \left| \frac{\psi_{n+1}}{\psi_n} \right|$$

which, in dynamical terms, is equivalent to the Lyapunov exponent of the Hamiltonian map (11), i.e.,

$$\lambda = \lim_{N \rightarrow \infty} \frac{1}{2Na} \sum_{n=1}^N \log \left(\frac{J_{n+1}}{J_n} \right) = \frac{1}{2a} \langle \log D_n^2 \rangle. \quad (17)$$

To compute the Lyapunov exponent (17) we expand the logarithm; within the second-order approximation one obtains

$$\begin{aligned} \lambda = & \frac{1}{2a} \left\langle \sin(2\theta_n + ka) \tilde{u}_n - \sin(2\theta_n + 2ka) \tilde{\Delta}_n \right. \\ & + \frac{1}{4} [1 - 2 \cos(2\theta_n + ka) + \cos(4\theta_n + 2ka)] \tilde{u}_n^2 \\ & + \frac{1}{4} [1 - 2 \cos(2\theta_n + 2ka) + \cos(4\theta_n + 4ka)] \tilde{\Delta}_n^2 \\ & \left. - \frac{1}{2} [\cos(ka) - 2 \cos(2\theta_n + 2ka) + \cos(4\theta_n + 3ka)] \tilde{u}_n \tilde{\Delta}_n \right\rangle \end{aligned} \quad (18)$$

The terms in the angular brackets of the right-hand side (rhs) of Eq. (18) must be averaged over the angle variable with an appropriate distribution $\rho(\theta)$. Typically, one uses a flat distribution $\rho(\theta) = 1/(2\pi)$. In fact, it is easy to see that in the absence of disorder the Hamiltonian map (13) reduces to the form

$$\begin{aligned} J_{n+1} &= J_n \\ \theta_{n+1} &= \theta_n + ka. \end{aligned}$$

Hence the angle variable has a fast dynamics compared to the action variable and quickly assumes a uniform distribution of values in the interval $[0 : 2\pi]$.

This reasoning fails, however, when the rotation angle is either zero or a rational multiple of π . In the latter case the noiseless angular map has periodic orbits which manifest themselves in the form of a slight modulation of the invariant measure when a weak noise is switched on. In particular, when one has

$$ka = \frac{\pi}{n}$$

the uniform distribution of the angular variable is modified by a perturbative term proportional to $\cos(2n\theta)$ or $\sin(2n\theta)$. This modulation of the invariant measure alters the value of the inverse localisation length (18) only for $n = \pm 1$, and $n = \pm 2$, because only second- and fourth-order harmonics are present in the rhs of Eq. (18). The values $ka = 0$ and $ka = \pm\pi$ correspond to the centre and the edges of the first Brillouin zone, i.e., to the edges of the energy bands. The values $ka = \pm\pi/2$ of the Bloch vector, on the other hand, correspond to values of the energy close to the band centre. For these special values of the rotation angle the assumption of a flat invariant distribution must be abandoned and the specific form of $\rho(\theta)$ has to be determined before one can compute the average in Eq. (18). The non-uniform distribution of the angular variable produces anomalies in the localisation length; we will analyse them elsewhere.

Except for the special cases mentioned above, one can compute the averages in Eq. (18) with a uniform angular distribution. The corresponding result is

$$\begin{aligned} \lambda &= \frac{1}{8a} \left[\langle \tilde{u}_n^2 \rangle + \langle \tilde{\Delta}_n^2 \rangle - 2 \langle \tilde{u}_n \tilde{\Delta}_n \rangle \cos(ka) \right] \\ &+ \frac{1}{2a} \left[\langle \tilde{u}_n \sin(2\theta_n + ka) \rangle - \langle \tilde{\Delta}_n \sin(2\theta_n + 2ka) \rangle \right]. \end{aligned} \quad (19)$$

To proceed further, we need to compute the noise-angle correlators which appear in formula (19). One can generalise the method used in [2] and introduce the correlator between the kick strength and the angle

$$r_l = \langle \tilde{u}_n \exp(i2\theta_{n-l}) \rangle$$

as well as the correlator between the kick timing and the angle

$$s_l = \langle \tilde{\Delta}_n \exp(i2\theta_{n-l}) \rangle.$$

Both correlators satisfy recursive relations, which can be derived as follows. Keeping only second-order terms in the disorder strength, one can write r_{l-1} in the form

$$\begin{aligned} r_{l-1} &= \left\langle \tilde{u}_n \exp(i2\theta_{n-l+1}) \right\rangle = \left\langle \tilde{u}_n \exp(i2\theta_{n-l}) \exp(i2ka) \right. \\ &\times \left. \left\{ 1 - i[1 - \cos(2\theta_{n-l} + ka)] \tilde{u}_{n-l} + i[\zeta - \cos(2\theta_{n-l} + 2ka)] \tilde{\Delta}_{n-l} \right\} \right\rangle. \end{aligned} \quad (20)$$

For weak disorder the triple and quadruple noise-angle correlators can be factorised and averages over the angle variable can be carried out with a uniform distribution. The result is

$$r_{l-1} = r_l \exp(i2ka) + \frac{i}{2} \exp(ika) \langle \tilde{u}_n \tilde{u}_{n-l} \rangle - \frac{i}{2} \langle \tilde{u}_n \tilde{\Delta}_{n-l} \rangle.$$

Multiplying both members of this identity by $\exp[i2ka(l-1)]$ and summing over l from zero to infinity, one obtains

$$r_0 = \frac{i}{2} \exp(-ika) \sum_{l=1}^{\infty} \langle \tilde{u}_n \tilde{u}_{n-l} \rangle \exp(i2kal) - \frac{i}{2} \exp(-i2ka) \sum_{l=1}^{\infty} \langle \tilde{u}_n \tilde{\Delta}_{n-l} \rangle \exp(i2kal).$$

From this expression one can easily compute the correlator between the angle and the kick strength in Eq. (19); in fact, one has

$$\begin{aligned} \langle \tilde{u}_n \sin(2\theta_n + ka) \rangle &= \text{Im}[r_0 \exp(ika)] \\ &= \frac{1}{2} \sum_{l=1}^{\infty} \langle \tilde{u}_n \tilde{u}_{n-l} \rangle \cos(2kal) - \frac{1}{2} \sum_{l=1}^{\infty} \langle \tilde{u}_n \tilde{\Delta}_{n-l} \rangle \cos[ka(2l-1)]. \end{aligned} \quad (21)$$

Following the same approach, one obtains that the correlator between the angle and the timing of the kick is

$$\begin{aligned} \langle \tilde{\Delta}_n \sin(2\theta_n + 2ka) \rangle &= \text{Im}[s_0 \exp(i2ka)] \\ &= \frac{1}{2} \sum_{l=1}^{\infty} \langle \tilde{\Delta}_n \tilde{u}_{n-l} \rangle \cos[ka(2l+1)] - \frac{1}{2} \sum_{l=1}^{\infty} \langle \tilde{\Delta}_n \tilde{\Delta}_{n-l} \rangle \cos(2kal). \end{aligned} \quad (22)$$

Plugging the noise-angle correlators (21) and (22) in Eq. (19), one obtains that the Lyapunov exponent is

$$\lambda = \frac{1}{8a} \left[\langle \tilde{u}_n^2 \rangle W_1(ka) + \langle \tilde{\Delta}_n^2 \rangle W_2(ka) - 2 \langle \tilde{u}_n \tilde{\Delta}_n \rangle \cos(ka) W_3(ka) \right] \quad (23)$$

where the functions $W_i(ka)$, defined by the identities

$$\begin{aligned} W_1(ka) &= 1 + 2 \sum_{l=1}^{\infty} \frac{\langle u_n u_{n+l} \rangle}{\langle u_n^2 \rangle} \cos(2kal) \\ W_2(ka) &= 1 + 2 \sum_{l=1}^{\infty} \frac{\langle \Delta_n \Delta_{n+l} \rangle}{\langle \Delta_n^2 \rangle} \cos(2kal) \\ W_3(ka) &= 1 + 2 \sum_{l=1}^{\infty} \frac{\langle u_n \Delta_{n+l} \rangle}{\langle u_n \Delta_n \rangle} \cos(2kal), \end{aligned} \quad (24)$$

are the Fourier transforms of the normalised binary correlators (5). Eq. (23), first derived in [9], shows that the Lyapunov exponent is the sum of three terms, with the first two addends describing the effects of purely compositional and structural disorder, while the third term is due to the interplay between these two kinds of randomness.

We stress that expression (23) is valid for every value of the energy within the allowed energy bands, with the exception of small neighbourhoods at the band edges (i.e., for $ka \simeq 0$ and $ka \simeq \pm\pi$) and close to the band centre (i.e., for $k \simeq \pi/2a$).

3 Designed mobility edges

3.1 Generation of self- and cross-correlated disorders

In this section we discuss how specific long-range self-correlations of the disorder can weaken or enhance the localisation of the electronic states and produce pre-defined mobility edges. We then analyse the additional effects of the cross-correlations between compositional and structural disorders. Formula (23) shows that the localisation length diverges in the energy intervals where the power spectra (24) vanish. The problem, therefore, is to generate two successions of random variables $\{u_n\}$ and $\{\Delta_n\}$ with self- and cross-correlators such that the power spectra (24) vanish in pre-assigned energy windows. We are dealing with an “inverse” problem which, as such, has no unique solution. Here we propose one, defining an algorithm for the construction of two successions $\{u_n\}$ and $\{\Delta_n\}$ with the required features.

As a first step, we consider two successions $\{X_n^{(1)}\}$ and $\{X_n^{(2)}\}$ of independent random variables with zero mean and unit variance. In other words, we require that

$$\langle X_n^{(i)} \rangle = 0 \quad \text{and} \quad \langle X_n^{(i)} X_m^{(j)} \rangle = \delta_{ij} \delta_{nm}$$

for $i, j = 1, 2$ and $n, m \in \mathbf{Z}$. In terms of these variables, we can construct two inter-correlated successions

$$\begin{aligned} Y_n^{(1)} &= X_n^{(1)} \cos \eta + X_n^{(2)} \sin \eta \\ Y_n^{(2)} &= X_n^{(1)} \sin \eta + X_n^{(2)} \cos \eta \end{aligned} \tag{25}$$

with η being a real parameter which determines the degree of inter-correlation

of the Y variables. In fact, one has

$$\langle Y_n^{(i)} \rangle = 0 \quad \text{and} \quad \langle Y_n^{(i)} Y_m^{(j)} \rangle = \delta_{nm} [\delta_{ij} + (1 - \delta_{ij}) \sin(2\eta)]$$

and this shows that the natural range of variation of the parameter η is the interval $[-\pi/4, \pi/4]$ with $\eta = \pi/4$ corresponding to total correlation of the $Y_n^{(1)}$ and $Y_n^{(2)}$ variables and $\eta = -\pi/4$ to total anticorrelation (for $\eta = 0$ no cross-correlations exist).

The next step consists in “filtering” the cross-correlated white-noise successions $\{Y_n^{(1)}\}$ and $\{Y_n^{(2)}\}$ in order to obtain two cross- and self-correlated sequences $\{u_n\}$ and $\{\Delta_n\}$. For this purpose we express the u_n and Δ_n random variables as convolution products of the form

$$u_n = \sum_{k=-\infty}^{\infty} \alpha_k Y_{n-k}^{(1)} \quad \text{and} \quad \Delta_n = \sum_{k=-\infty}^{\infty} \beta_k Y_{n-k}^{(2)}. \quad (26)$$

and we look for appropriate successions of the coefficients α_k and β_k . We suppose that $\alpha_k = \alpha_{-k}$ and $\beta_k = \beta_{-k}$. Starting from Eq. (26) one obtains that the average values of the variables u_n and Δ_n vanish

$$\langle u_n \rangle = 0 \quad \text{and} \quad \langle \Delta_n \rangle = 0$$

and that the binary correlators take the values

$$\langle u_n u_{n+k} \rangle = \sum_{l=-\infty}^{\infty} \alpha_l \alpha_{l+k}, \quad (27)$$

$$\langle \Delta_n \Delta_{n+k} \rangle = \sum_{l=-\infty}^{\infty} \beta_l \beta_{l+k}, \quad (28)$$

$$\langle \Delta_n u_{n+k} \rangle = \langle u_n \Delta_{n+k} \rangle = \sum_{l=-\infty}^{\infty} \alpha_l \beta_{l+k} \sin(2\eta). \quad (29)$$

Comparing Eqs. (27) and (28) with the binary self-correlators in Eq. (5), one arrives at the equations

$$\begin{aligned} \sum_{l=-\infty}^{\infty} \alpha_l \alpha_{l+k} &= \langle u_n^2 \rangle \chi_1(k) \\ \sum_{l=-\infty}^{\infty} \beta_l \beta_{l+k} &= \langle \Delta_n^2 \rangle \chi_2(k) \end{aligned}$$

whose solution is

$$\begin{aligned}\alpha_k &= \frac{2}{\pi} \int_0^{\pi/2} \sqrt{\langle u_n^2 \rangle W_1(x)} \cos(2kx) dx, \\ \beta_k &= \frac{2}{\pi} \int_0^{\pi/2} \sqrt{\langle \Delta_n^2 \rangle W_2(x)} \cos(2kx) dx.\end{aligned}\tag{30}$$

Inserting the coefficients (30) in the convolution products (26) one obtains random variables $\{u_n\}$ and $\{\Delta_n\}$ with zero average and pre-assigned self-correlators $\chi_1(k)$ and $\chi_2(k)$, as required. To complete the picture, one should specify the inter-correlation parameter η which, together with the coefficients (30) defines the cross-correlator (29).

Thus, we have obtained a recipe that gives two random successions $\{u_n\}$ and $\{\Delta_n\}$ in terms of the pre-defined normalised self-correlators $\chi_1(k)$ and $\chi_2(k)$, or, equivalently, of the pre-assigned power spectra $W_1(ka)$ and $W_2(ka)$ and of the inter-correlation parameter η . We can now see what is the form of the inverse localisation length (23) when the random variables u_n and Δ_n are generated with the above-described method. After some algebra, one can write the cross power spectrum as

$$W_3(ka) = \frac{\sqrt{\langle u_n^2 \rangle W_1(ka) \langle \Delta_n^2 \rangle W_2(ka)}}{\langle u_n \Delta_n \rangle} \sin(2\eta).$$

Inserting this result in expression (23) one obtains

$$\begin{aligned}\lambda &= \frac{1}{8a} \left[\langle \tilde{u}_n^2 \rangle W_1(ka) + \langle \tilde{\Delta}_n^2 \rangle W_2(ka) \right. \\ &\quad \left. - 2\sqrt{\langle \tilde{u}_n^2 \rangle \langle \tilde{\Delta}_n^2 \rangle W_1(ka) W_2(ka)} \cos(ka) \sin(2\eta) \right].\end{aligned}\tag{31}$$

3.2 Numerical examples

To test the validity of formula (31) we construct a pair of random sequences $\{u_n\}$ and $\{\Delta_n\}$ which enhance the localisation of the states in two energy windows $[q_1^2, q_2^2]$ and $[q_3^2, q_4^2]$ and delocalise the states in the rest of the band. For the sake of simplicity we consider compositional and structural disorders with identical self-correlators of the form

$$\chi_1(n) = \chi_2(n) = \frac{1}{2(k_2 - k_1)an} [\sin(2k_2an) - \sin(2k_1an)]\tag{32}$$

The power-law decay of this function is the signature of long-range auto-correlations of the disorder. The correlators (32) correspond to the power spectra

$$W_1(ka) = W_2(ka) = \begin{cases} \frac{\pi}{2a(k_2 - k_1)} & \text{if } k \in [k_1, k_2] \\ 0 & \text{if } k \in [0, k_1] \cup [k_2, \frac{\pi}{2a}] \end{cases}. \quad (33)$$

In Eqs. (32) and (33), k_1 and k_2 represent the two Bloch vectors corresponding to the mobility edges q_1^2 and q_2^2 , i.e.,

$$q(k_1) = q_1 \quad \text{and} \quad q(k_2) = q_2.$$

Note that the power spectra (24) are periodic functions of period $\pi/2a$ and therefore it is enough to define them in the interval $[0, \pi/2a]$.

For our first numerical example we chose disorder strengths equal to $\sqrt{\langle u_n^2 \rangle} = \sqrt{\langle \Delta_n^2 \rangle} = 0.04$ and a mean field value $U = 0.7$. We considered two Bloch vectors $k_1 = \pi/5a$ and $k_2 = 2\pi/5a$, which, for the given value of U , correspond to mobility edges at

$$\tilde{q}_1 = 0.327, \quad \tilde{q}_2 = 0.476, \quad \tilde{q}_3 = 0.652, \quad \tilde{q}_4 = 0.838$$

with $\tilde{q}_i = q_i/\pi$. Note that, with our choice of U , the propagation wavevector q within the first energy bands spans the interval ranging from $q_l/\pi = 0.259$ to $q_r/\pi = 1.0$. Fig. 1 shows that the theoretical predictions of Eq. (31) are well-matched by the numerical results. As expected, the long-range self-correlations (32) produce sharp mobility edges, whereas the cross-correlations can substantially change the spatial extension of the localised states. In Fig. (1) the case without cross-correlations ($\eta = 0$) is compared with the two extreme cases of total positive ($\eta = \pi/4$) and negative ($\eta = -\pi/4$) cross-correlations.

As a second example, in Fig. 2 we represent the theoretical predictions and numerical results for the complementary case, characterised by the same mobility edges of the previous example but with inverted windows of localised and delocalised states. (The values of the disorder strengths and of the mean field are the same as in the previous case.) We observe again a good correspondence between the numerical values and the inverse localisation length (31).

To conclude this section, we observe that the spatial extension of the localised states can be significantly reduced by squeezing the energy windows

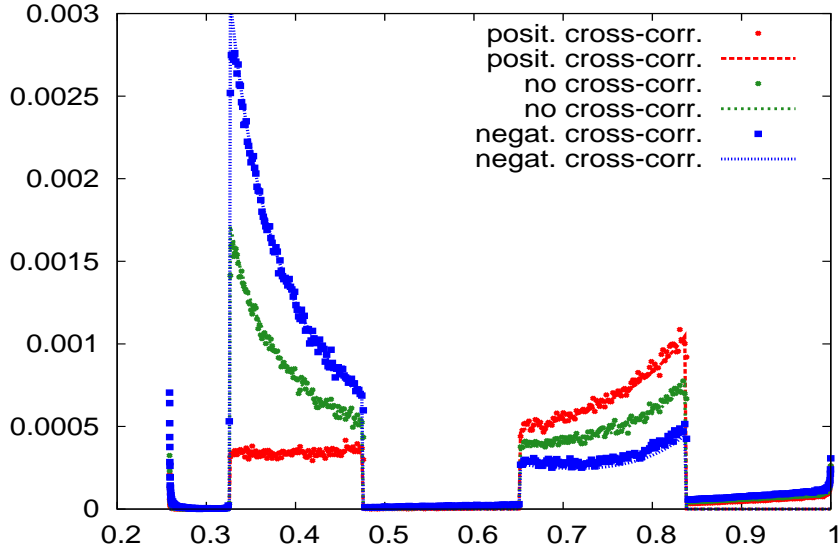


Figure 1: Inverse localisation length versus q/π . Lines correspond to the predictions of Eq. (31); the symbols to numerical results.

of localised states. This localisation enhancement, first discussed in [5], is a consequence of the normalisation condition

$$\int_0^{\pi/(2a)} W_i(ka) dk = \frac{\pi}{2a},$$

which follows from the fact that $\chi_i(0) = 1$. To illustrate this effect, we consider a third example, with all parameters unchanged with respect to the first one ($U = 0.7$, $\sqrt{\langle u_n^2 \rangle} = \sqrt{\langle \Delta_n^2 \rangle} = 0.04$) except for the size of the windows of localised states, which we shrink by setting $k_1 = 0.29\pi/a$ and $k_2 = 0.31\pi/a$. In terms of the propagation wavevector, these values of the Bloch vectors correspond to mobility edges at

$$\tilde{q}_1 = 0.388, \quad \tilde{q}_2 = 0.402, \quad \tilde{q}_3 = 0.736, \quad \tilde{q}_4 = 0.755. \quad (34)$$

The theoretical and numerical results for the inverse localisation length, represented in Fig. 3, display a clear enhancement of localisation in the narrowed energy intervals of localised states. The stronger localisation magnifies the effect of the cross-correlations of the compositional and structural disorder,

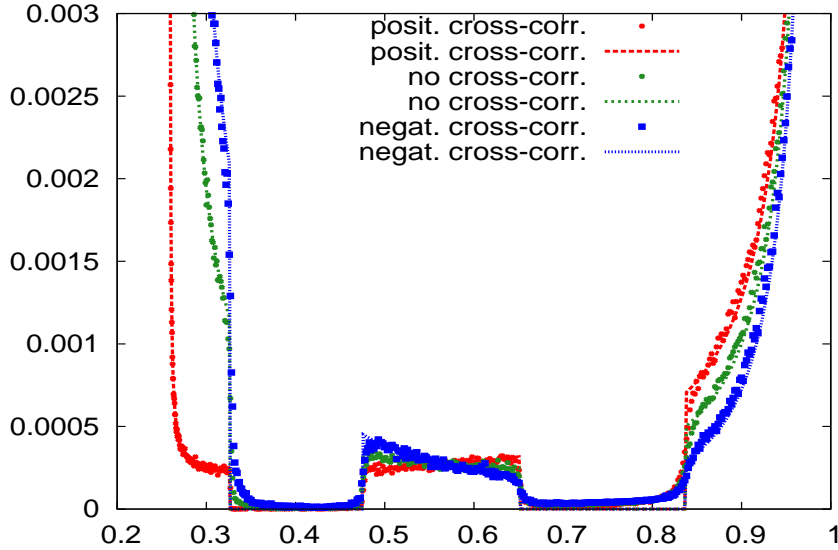


Figure 2: Inverse localisation length versus q/π . Lines correspond to theoretical predictions and symbols to numerical results.

enlarging the difference between the extreme cases of total positive and negative inter-correlations.

4 Transport properties

In the previous sections we have considered the structure of the electronic states in a infinite Kronig-Penney model. We now turn our attention to the relevant problem of electronic transmission through finite disordered segments. We consider the case of a random Kronig-Penney model extending over N lattice sites sandwiched between two semi-infinite perfect leads. From the mathematical point of view, this means that the variables u_n and Δ_n in the Schrödinger equation (1) are defined as before for $1 \leq n \leq N$, but vanish for $n < 1$ and $n > N$. We assume that the left lead carries an incoming and a reflected wave with wavevector q ,

$$\psi_n = e^{iqan} + re^{-iqan} \quad \text{for } n = 0, -1, -2, \dots$$

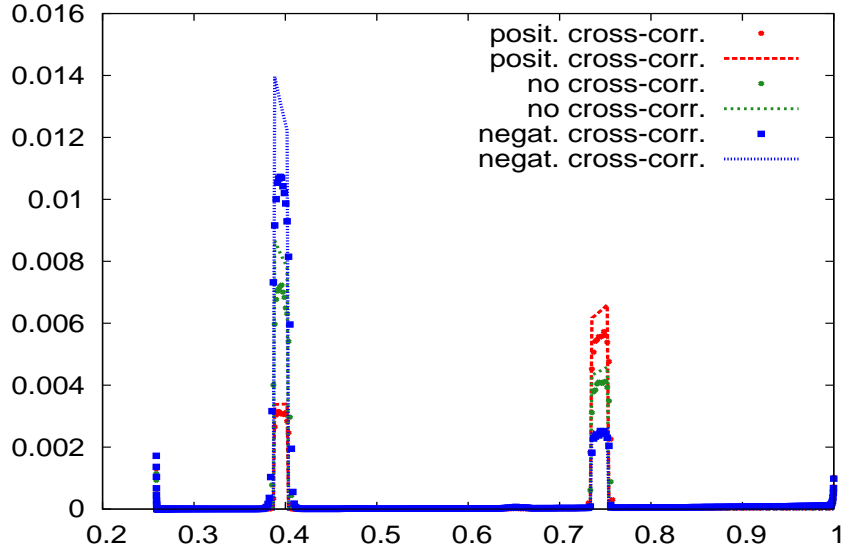


Figure 3: Inverse localisation length versus q/π . Lines correspond to theoretical predictions and symbols to numerical results.

while a transmitted wave propagates in the right lead

$$\psi_n = t e^{i q a n} \quad \text{for} \quad n = N + 1, N + 2, \dots$$

To determine the transmission coefficient $T(q) = |t(q)|^2$ we follow the variant of the transfer-matrix approach introduced in [12]. After eliminating the momenta from the map (7), with the obvious substitution $x_n \rightarrow \psi_n$ we obtain the equation

$$\begin{aligned} & \frac{1}{\sin [q (a + \Delta_n)]} \psi_{n+1} + \frac{1}{\sin [q (a + \Delta_{n-1})]} \psi_{n-1} \\ &= \left\{ \cot [q (a + \Delta_n)] + \cot [q (a + \Delta_{n-1})] + \frac{1}{q} (U + u_n) \right\} \psi_n, \end{aligned} \quad (35)$$

which defines the tight-binding system corresponding to the Kronig-Penney model (1). Note that the compositional disorder in the Kronig-Penney model manifests itself as diagonal disorder in Eq. (35), whereas the structural disorder shows up in both the diagonal and off-diagonal random coefficients of the tight-binding model (35). Using the transfer-matrix formalism, one can

write Eq. (35) in the form

$$\begin{pmatrix} \psi_{n+1} \\ \psi_n \end{pmatrix} = \mathbf{M}_n \begin{pmatrix} \psi_n \\ \psi_{n-1} \end{pmatrix} \quad (36)$$

with the elements of the matrix \mathbf{M}_n being

$$\begin{aligned} (\mathbf{M}_n)_{11} &= \left\{ \cot [q (a + \Delta_n)] + \cot [q (a + \Delta_{n-1})] + \frac{1}{q} (U + u_n) \right\} \sin [q (a + \Delta_n)], \\ (\mathbf{M}_n)_{12} &= -\frac{\sin [q (a + \Delta_n)]}{\sin [q (a + \Delta_{n-1})]}, \\ (\mathbf{M}_n)_{21} &= 1, \\ (\mathbf{M}_n)_{22} &= 0. \end{aligned}$$

The total transfer matrix connecting the wavefunctions in the two leads is then

$$\mathbf{M} = \mathbf{M}_N \mathbf{M}_{N-1} \cdots \mathbf{M}_1. \quad (37)$$

Following Pichard [13], one can write the transmission coefficient in terms of the elements of the matrix (37). One thus obtains the expression

$$T_N(q) = \frac{4 \sin^2(q) (\det \mathbf{M})^2}{|\mathbf{M}_{21} - \mathbf{M}_{12} + \mathbf{M}_{22} e^{iq} - \mathbf{M}_{11} e^{-iq}|^2}. \quad (38)$$

We remark that the factor $(\det \mathbf{M})^2$ enters the previous formula because the determinant of the transfer matrices \mathbf{M}_n is not unitary. More precisely, one has

$$\det \mathbf{M} = \frac{\sin [q (a + \Delta_N)]}{\sin [q (a + \Delta_0)]}.$$

To avoid the nuisance of a total transfer matrix with non-unitary determinant, one can redefine the random barrier as including an extra site with no disorder on each side. From now on we will adopt this convention and drop the determinant factor in formulae derived from Eq. (38).

To express the transmission coefficient (38) in a more convenient way, we perform a similarity transformation

$$\mathbf{Q}_n = \mathbf{R} \mathbf{M}_n \mathbf{R}^{-1}$$

with

$$\mathbf{R} = \begin{pmatrix} 1 & 0 \\ \cos(qa) / \sin(qa) & -1 / \sin(qa) \end{pmatrix}$$

and put the map (36) in the equivalent form

$$\begin{pmatrix} x_{n+1} \\ p_{n+1} \end{pmatrix} = \mathbf{Q}_n \begin{pmatrix} x_n \\ p_n \end{pmatrix}. \quad (39)$$

This allows one to cast the transmission coefficient (38) in the more appealing form [12]

$$T_N(q) = \frac{4}{2 + \mathbf{v}_1 \cdot \mathbf{v}_1 + \mathbf{v}_2 \cdot \mathbf{v}_2}, \quad (40)$$

with \mathbf{v}_1 and \mathbf{v}_2 being the two-component vectors defined as

$$\mathbf{v}_1 = \mathbf{Q}_{N+1} \mathbf{Q}_N \cdots \mathbf{Q}_1 \mathbf{Q}_0 \begin{pmatrix} 1 \\ 0 \end{pmatrix}$$

and

$$\mathbf{v}_2 = \mathbf{Q}_{N+1} \mathbf{Q}_N \cdots \mathbf{Q}_1 \mathbf{Q}_0 \begin{pmatrix} 0 \\ 1 \end{pmatrix}.$$

Eq. (40) is very convenient for the numerical evaluation of the transmission coefficient, which can be efficiently determined by computing the evolution of the initial vectors $(1, 0)$ and $(0, 1)$ under the map (39).

Using this approach, we numerically investigated the effects of the long-range correlations of the disorder on the transmission coefficient $T_N(q)$. In the absence of cross-correlations, only two length scales are relevant for the transport properties of the disordered segment, namely, the length of the segment itself, $L = Na$ and the spatial extension l_{loc} of the localised states in the infinite random model. In principle one should also consider the localisation length l_{del} of the delocalised states, because the vanishing of the second-order Lyapunov exponent (23) does not necessarily imply that the higher-order terms must also be zero. However, for weak disorder the spatial extension of the delocalised states is so large that it can be considered as infinite with respect to the length L of the random barrier.

In the localised regime, i.e., when the condition $l_{\text{loc}} \ll L$ is fulfilled, our numerical experiments show that the windows of delocalised states created by long-ranged self-correlations of the disorder survive in the case of disordered segments, where they manifest themselves as energy windows with transmittivity close to one. This agrees with the results already obtained, both numerically and experimentally, for barriers with purely compositional or structural disorder [3, 8]. Our numerical data also show that the cross-correlations of the disorder have additional effects on the transport properties. Their influence is most evident in the localisation windows created by

long-ranged self-correlations of the disorder, where cross-correlations either enhance or diminish the electronic transmission according to whether they increase or decrease the localisation length.

The effects of both the self- and the cross-correlations of the disorder can be appreciated in Figs. 4 and 5, which represent the transmission amplitude for two lengths of a random sample with the same disorder characteristics of the third example analysed in Sec. 3.2. In other words, we consider a random Kronig-Penney barrier with mean field $U = 0.7$, disorder strengths $\sqrt{\langle u_n^2 \rangle} = \sqrt{\langle \Delta_n^2 \rangle} = 0.04$, and windows of localised states $[q_1, q_2]$ and $[q_3, q_4]$, with edges defined by Eq. (34). Each figure represents the transmission coefficients for the cases of total positive and negative cross-correlations.

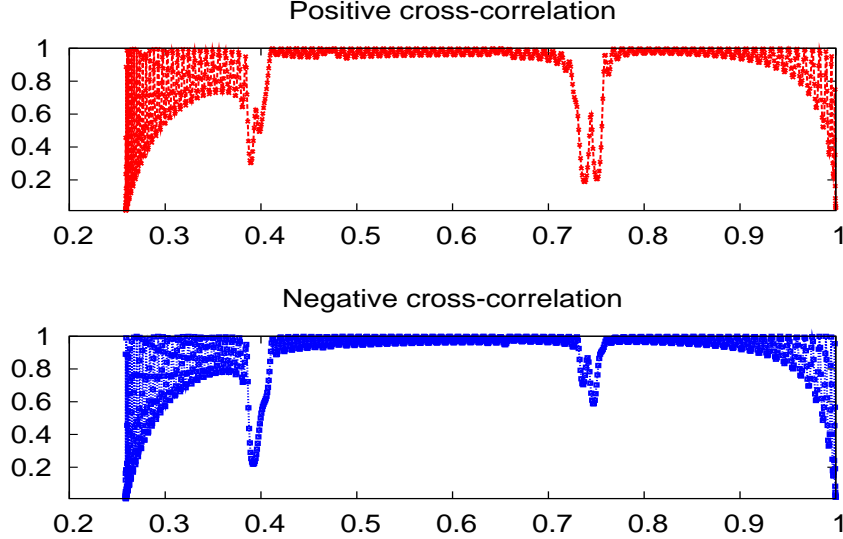


Figure 4: Transmission coefficient $T_N(q)$ versus q/π for random sample of $N = 100$ sites.

When the cross-correlations are taken into account, it is better to characterise the spatial extension of the localised states in terms not of one but of two length scales, i.e., $l_{\text{loc}}^+(q)$ and $l_{\text{loc}}^-(q)$, which correspond to the maximum and minimum values of the localisation length obtained by varying the inter-correlation of the compositional and structural disorders. In the present case, one has $l_{\text{loc}}^- \sim 100a$ and $l_{\text{loc}}^+ \sim 300a$ in the localisation window of lower

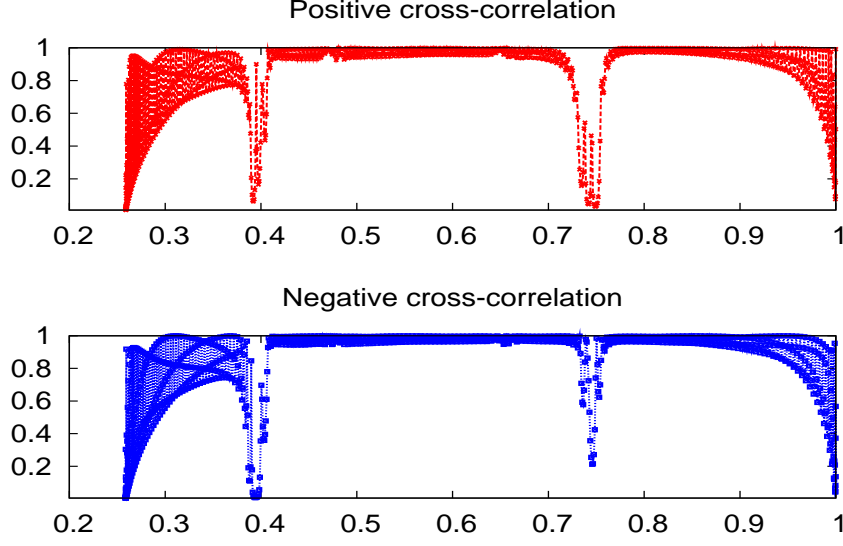


Figure 5: Transmission coefficient $T_N(q)$ versus q/π for random sample of $N = 200$ sites.

energy and $l_{\text{loc}}^- \sim 200a$ and $l_{\text{loc}}^+ \sim 400a$ in the higher-energy localisation window. The data represented in Figs. 4 and 5 were obtained for the sample lengths $L = 100a$ and $L = 200a$, which correspond to the intermediate region between the ballistic regime, characterised by $L \ll l_{\text{loc}}^-$ and the exponentially localised regime for which $l_{\text{loc}}^+ \ll L$.

Two main features emerge from the numerical data. On the one hand, as L is increased the mobility edges become sharper and sharper, because the localisation of the electronic state in the windows $[q_1, q_2]$ and $[q_3, q_4]$ becomes more and more effective. On the other hand, the existence of two localisation lengths implies that the regime of exponential localisation is attained with different speed according to the type and degree of cross-correlations. This is the physical origin of the difference in the transmission coefficients for positive and negative cross-correlations.

In general terms, one should notice that, when the length of the sample is less than the minimum localisation length l_{loc}^- , the localisation of the electronic states is very weak, and this can produce strong sample-to-sample fluctuations of the transmission coefficient which partially mask the effects of cross-correlations. As the length of the barrier is increased, these effects

become clearly discernible and their influence peaks in the intermediate region between the ballistic and the localised regimes. If one lets the length of the random sample grow further, the regime of exponential localisation is eventually reached for both kinds of cross-correlations. In this regime both transmission coefficients are exponentially small in the localisation windows and their absolute difference is therefore hard to detect.

5 Conclusions

In this paper we have analysed the structure of the electronic states and transport properties of a Kronig-Penney model with weak compositional and structural disorder. We have shown that specific long-range self-correlations of the disorder can enhance or suppress the localisation of the electronic states in pre-defined energy windows and that an additional modulation of the localisation length can be obtained by cross-correlating the two kinds of disorder. A method to generate compositional and structural disorder with arbitrary self- and cross-correlations has been given.

The analysis performed in the second part of this work shows that, by carefully selecting the statistical properties of the disorder, one can produce random samples with peculiar transport properties. In particular, it is possible to obtain almost perfect transmission in pre-defined energy windows. Although self-correlations play a dominant role in shaping the transport properties of finite-size random chains, cross-correlations can be used to fine-tune the transmission coefficient.

J. C. H.-H. and L.T. gratefully acknowledge the support of the CONACyT grant nr. 84604 and of the CIC-2009 grant (Universidad Michoacana). The work of F.M.I. was partly supported by the CONACyT grant nr. 80715.

References

- [1] F. A. B. F. de Moura, M. L. Lyra, *Phys. Rev. Lett.*, **81**, 3735 (1998);
F. A. B. F. de Moura, M. L. Lyra, *Phys. Rev. Lett.*, **84**, 199 (2000);
F. A. B. F. de Moura, M. L. Lyra, *Physica A*, **266**, 465 (1999);
J. M. Luck, *Phys. Rev. B*, **39**, 5834 (1989)
- [2] F. M. Izrailev, A. A. Krokhin, *Phys. Rev. Lett.*, **82**, 4062 (1999);
A. A. Krokhin, F. M. Izrailev, *Ann. Phys. (Leipzig)* **SI-8**, 153 (1999);

- F. M. Izrailev, N. M. Makarov, *J. Phys. A: Math. Gen.*, **38**, 10613 (2005)
- [3] F. M. Izrailev, A. A. Krokhin, S. E. Ulloa, *Phys. Rev. B*, **63**, 041102(R) (2001)
- [4] U. Kuhl, F. M. Izrailev, A. A. Krokhin, H.-J. Stöckmann, *Appl. Phys. Lett.*, **77**, 633 (2000); A. Krokhin, F. Izrailev, U. Kuhl, H.-J. Stöckmann, S. E. Ulloa, *Physica E*, **13**, 695 (2002)
- [5] U. Kuhl, F. M. Izrailev, A. A. Krokhin, *Phys. Rev. Lett.* **100**, 126402 (2008)
- [6] R. de L. Kronig, W. G. Penney, *Proc. Roy. Soc. (Series A)* **130**, 499 (1931)
- [7] J. H. Davies, *The physics of low-dimensional semiconductors: an introduction*, Cambridge University Press, Cambridge (1998)
- [8] G. A. Luna-Acosta, F. M. Izrailev, N. M. Makarov, U. Kuhl, H.-J. Stöckmann, *Phys. Rev. B*, **80**, 1151112 (2009)
- [9] J. C. Hernández Herrejón, F. M. Izrailev, L. Tessieri, *Physica E*, **40**, 3137-3140 (2008)
- [10] F. M. Izrailev, T. Kottos, G. P. Tsironis, *Phys. Rev. B*, **52**, 3274 (1995)
- [11] F. M. Izrailev, S. Ruffo, L. Tessieri, *J. Phys. A: Math. Gen.*, **31**, 5263 (1998)
- [12] T. Kottos, G. P. Tsironis, F. M. Izrailev, *J. Phys.: Condens. Matter*, **9**, 1777-1791 (1997)
- [13] J. L. Pichard, *J. Phys. C: Solid State Physics*, **19**, 1519 (1986)